ACS APPLIED MATERIALS & INTERFACES

www.acsami.org

Research Article

Targeting and Inhibiting *Plasmodium falciparum* Using Ultra-small Gold Nanoparticles

Silvia Varela-Aramburu,[‖] Chandradhish Ghosh,[‖] Felix Goerdeler, Patricia Priegue, Oren Moscovitz, and Peter H. Seeberger*

Cite This: *ACS Appl. Mater. Interfaces* 2020, 12, 43380–43387

Read Online

ACCESS | Metrics & More | Article Recommendations | Supporting Information

ABSTRACT: Malaria, a mosquito-borne disease caused by *Plasmodium* species, claims more than 400,000 lives globally each year. The increasing drug resistance of the parasite renders the development of new anti-malaria drugs necessary. Alternatively, better delivery systems for already marketed drugs could help to solve the resistance problem. Herein, we report glucose-based ultra-small gold nanoparticles (Glc-NCs) that bind to cysteine-rich domains of *Plasmodium falciparum* surface proteins. Microscopy shows that Glc-NCs bind specifically to extracellular and all intra-erythrocytic stages of *P. falciparum*. Glc-NCs may be used as drug delivery agents as illustrated for ciprofloxacin, a poorly soluble antibiotic with low antimalarial activity. Ciprofloxacin conjugated to Glc-NCs is more water-soluble than the free drug and is more potent. Glyco-gold nanoparticles that target cysteine-rich domains on parasites may be helpful for the prevention and treatment of malaria.

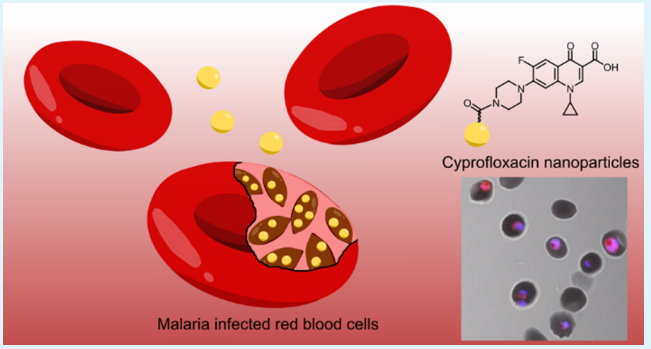

KEYWORDS: *gold nanoparticles, Plasmodium falciparum, targeting, ciprofloxacin, inhibition*

1. INTRODUCTION

Malaria is a mosquito-borne disease caused by protozoa of the genus *Plasmodium* that remains a significant health burden.[1] Five *Plasmodium* species can infect humans, but *Plasmodium falciparum* (*P. falciparum*) is the most severe one. Efforts toward malaria eradication have received much attention, while incorrect diagnosis and resistance to conventional drugs pose a major impediment. Resistance against all major classes of drugs, 4-aminoquinolines (chloroquine, amodiaquine, and piperaquine), antifolates, aryl amino-alcohols (quinine, lumefantrine, and mefloquine), artemisinin derivatives, antibiotics (clindamycin and doxycycline), and napthoquinone (atovaquone), has been reported.[2] New malarial therapy or drug delivery approaches using repurposed anti-infective drugs are also alternative treatment options.[3−5]

Malaria symptoms appear during the blood stage of the *P. falciparum* life cycle when merozoites are released from the liver into the bloodstream. These merozoites invade red blood cells (RBCs) and start a 48 h asexual developmental cycle through rings, trophozoites, and schizonts. During this blood life cycle, some of the parasites undergo gametocytogenesis, where they develop into gametocytes that are responsible for the transmission of the disease. Ideal drug delivery systems target all these stages in the host.

One drug delivery strategy is based on the incorporation of groups that bind to the targets on the parasite surface. The merozoite surface is coated with proteins mediating human erythrocyte invasion.[6] Many of these surface proteins contain cysteine-rich domains that play important roles during the invasion process, such as the reticulocyte binding homolog 5 (PfRh5), the cysteine-rich protective antigen (CyRPA), the erythrocyte-binding antigen-175 (EBA-175), the cysteine repeat modular proteins (PfPCRMP1-2), or the Duffy-binding-like erythrocyte-binding protein (DBL-EBP).[7−12] Cysteine-rich domains are also expressed on the surface of schizonts, gametocytes, and sporozoites *P. falciparum*.[6,13,14]

Thiols bind to gold nanoparticles to form strong bonds,[15] and gold nanoparticles have been functionalized with cysteine and used for cysteine detection.[16−21] We developed glucose-based ultra-small gold nanoparticles or gold nanoclusters (Glc-NCs) to target cysteine-rich proteins on the surface of *P. falciparum*. Glc-NCs were used without further functionalization or tagged with a dye to gain insight into the binding to different parasite stages. After specifically targeting intra-erythrocytic stages of *P. falciparum*, Glc-NCs were loaded

Received: May 18, 2020
Accepted: September 2, 2020
Published: September 2, 2020

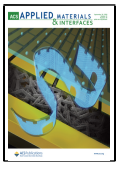

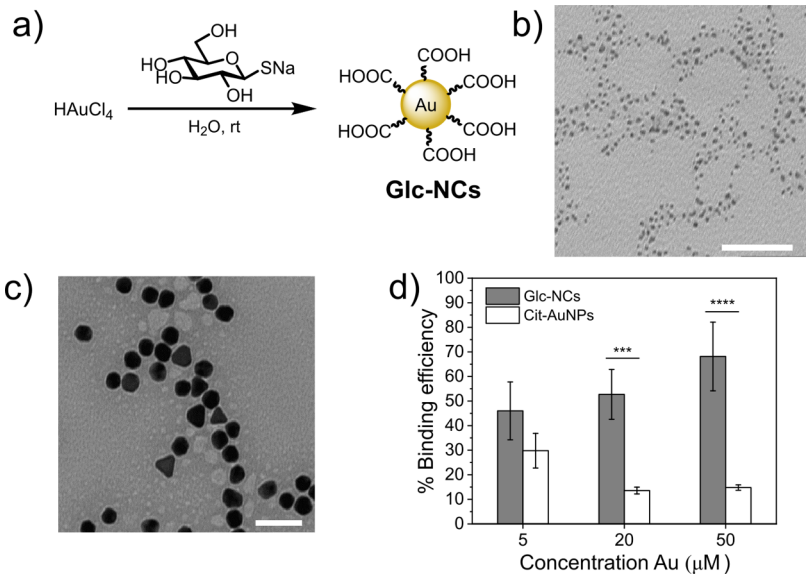

Figure 1. Synthesis, characterization, and binding efficiency of gold nanoparticles to extracellular malaria parasites. (a) Synthesis of Glc-NCs.[22] (b) TEM image of 2 nm Glc-NCs (scale bar: 50 nm). (c) TEM image of 20 nm Cit-AuNPs (scale bar: 50 nm). (d) ICP-AES detection of Au bound to extracellular parasites showed higher binding efficiency toward Glc-NCs when compared to Cit-AuNPs. ***$P \leq 0.001$; ****$P \leq 0.0001$.

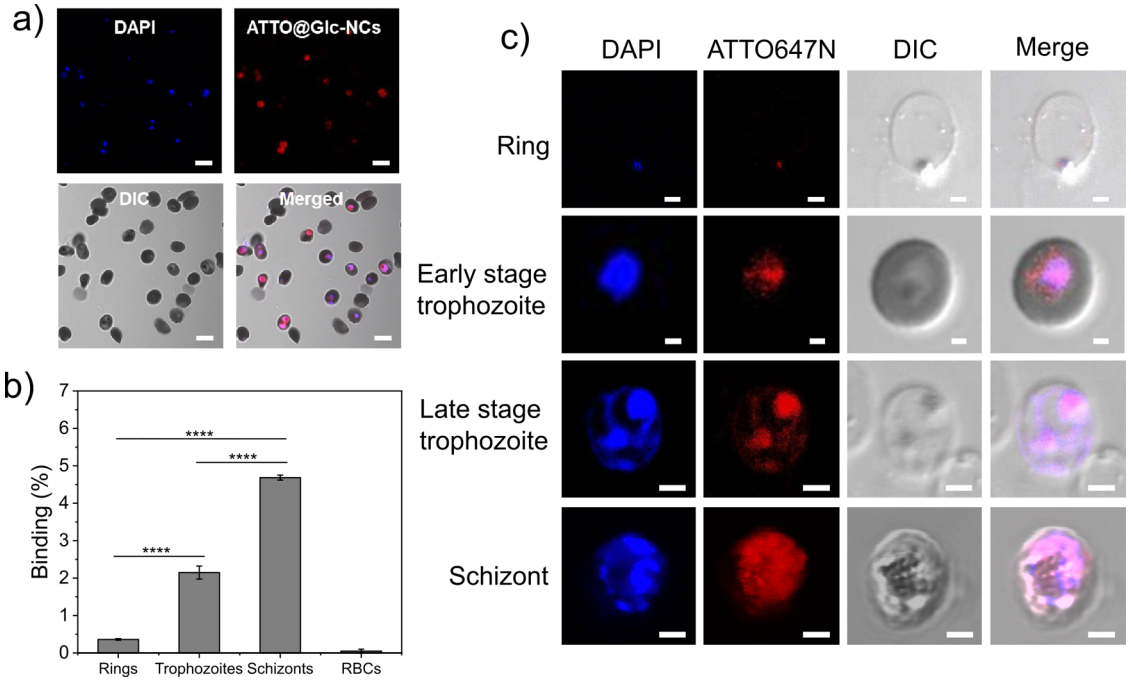

Figure 2. Analysis of the binding of Glc-NCs to different blood stages of *P. falciparum*. (a) CLSM imaging of ATTO@Glc-NCs incubated for 15 min with infected RBCs showed specific binding of intracellular *P. falciparum* (red channel, ATTO647N; blue channel, DAPI; scale bar: 5 μm). (b) FACS analysis of the binding of ATTO@Glc-NCs incubated for 15 min with highly synchronized *P. falciparum* cultures. Parasitemia was determined using SYBR Green (FITC channel), and ATTO647N dye was detected to determine the binding of ATTO@Glc-NCs (APC channel). ****$P \leq 0.0001$. (c) CLSM imaging of individual asexual erythrocyte stages incubated with ATTO@Glc-NCs showed specific binding for all the stages (red channel, ATTO647N (ATTO@Glc-NCs); blue channel, DAPI; scale bar: 2 μm).

with ciprofloxacin to explore the inhibitory effect on the parasites compared to the free drug. The significantly lower 50% inhibitory concentration (IC_{50}) value of the drug-loaded nanoparticles compared to the drug alone shows the therapeutic potential of using gold nanoparticles as drug delivery nanocarriers without the need for specific complex targeting functionalities.

2. RESULTS AND DISCUSSION

2.1. Binding Assessment of Gold Nanoparticles to Extracellular *P. falciparum* Parasites. *P. falciparum* was chosen as a model to assess whether gold nanoparticles are suitable to target cysteine-rich domains on surface proteins since the erythrocytic cycle involves invasion of RBCs that are not capable of performing endocytosis. *In vitro* experiments inspecting the different intracellular parasite stages are less

https://dx.doi.org/10.1021/acsami.0c09075
ACS Appl. Mater. Interfaces 2020, 12, 43380−43387

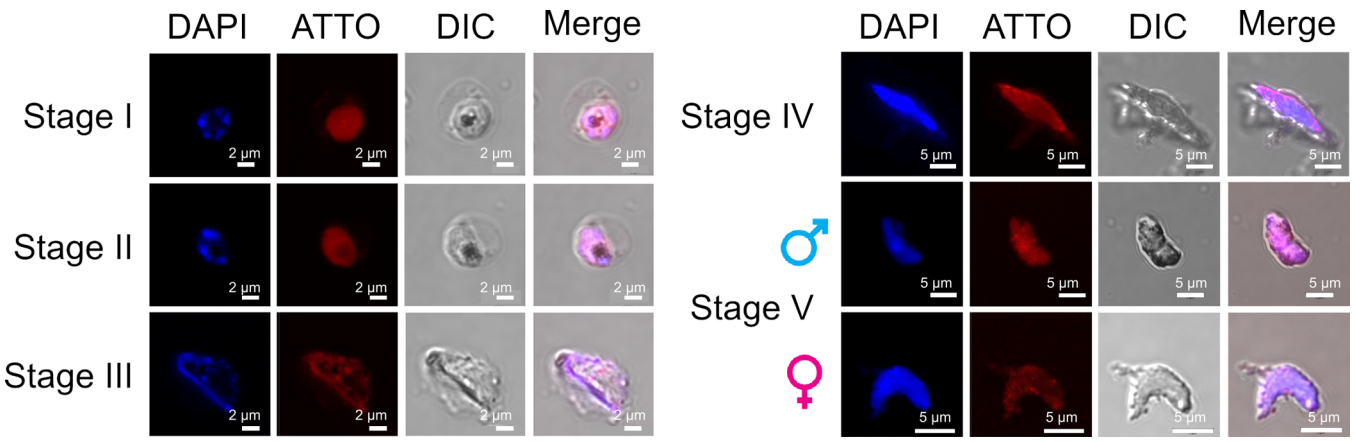

Figure 3. CLSM images of gametocyte blood stages of *P. falciparum* incubated with ATTO@Glc-NCs (red channel, ATTO647N (ATTO@Glc-NCs); blue channel, DAPI; left scale bars: 2 μm; right scale bars: 5 μm).

complicated when compared to other parasite models that require complex eukaryotic host cells. Initially, extracellular *P. falciparum* parasites were used to analyze the binding affinity toward gold nanoparticles of different sizes. For this, intracellular schizonts were treated with saponin to lyse the red blood cell hosts, leaving the mature extracellular parasites intact. We synthesized and characterized citrate-stabilized gold nanoparticles (Cit-AuNPs, 20 nm) and glucoside-based ultrasmall gold nanoparticles (Glc-NCs, 2 nm) (Figure 1a,b) to investigate binding to extracellular *P. falciparum*.[22] Both nanoparticle samples were incubated at three concentrations (5, 20, and 50 μM based on atomic gold) in PBS with extracellular parasites for 15 min and washed with PBS buffer to remove unbound nanoparticles. After treatment of the parasites with aqua regia, inductively coupled plasma with atomic emission spectrometry (ICP-AES) was used to determine the concentration of gold in the samples. Binding efficiency was further calculated based on the concentration of bound gold with respect to the concentration of gold added to the extracellular parasites. Both Cit-AuNPs and Glc-NCs were detected in the parasite samples, proving the existing binding affinity of the two gold nanoparticle samples toward extracellular mature *P. falciparum* parasites (Figure 1c). Glc-NCs bind much stronger than Cit-AuNPs. Possibly, the higher surface area of Glc-NCs (2 nm) compared to Cit-AuNPs (20 nm) led to an increased accumulation on the parasites. In addition, the hydroxyl groups of a glucose moiety stabilizing them might engage in hydrogen bonding interactions with the proteins.

2.2. Hemolytic Activity of Gold Nanoparticles. In order to investigate if Glc-NCs could traverse the RBC membrane and target the intracellular parasites, their hemolytic activity was assessed. Different concentrations of Glc-NCs were incubated with erythrocytes for 96 h but, even at the highest concentration tested (20 μM), no hemolysis was observed (Figure S1), demonstrating the safety of Glc-NCs to mammalian cells.

2.3. Targeting Asynchronous Intracellular *P. falciparum* Parasites Using Gold Nanoparticles. The affinity of Glc-NCs toward intracellular parasites was assessed. The stability of Glc-NCs in *P. falciparum* culture medium was investigated by TEM imaging. Overnight incubation of Glc-NCs in protein-rich medium showed a particle size ranging 2–5 nm (Figure S2a,b), proving that even though some nanoparticles showed a small increase in size, Glc-NCs were overall stable in growth medium. To detect the nanoparticles, Glc-NCs were first tagged with the ATTO647N dye by amidation using EDC/sulfo-NHS as coupling reagents to yield ATTO@Glc-NCs (Figure S3). The fluorescently tagged gold nanoparticles were then incubated for 15 min with asynchronous cultures of infected RBCs. Uninfected RBCs served as a control. The cultures were thoroughly washed and incubated with DAPI that stains the parasites, as it is a nucleic acid stain, but not RBCs that lack DNA. Confocal laser scanning microscopy (CLSM) showed that Glc-NCs were able to specifically bind intracellular *P. falciparum* (Figure 2a) but not RBCs (Figure S4a). Non-conjugated ATTO647N dye was also incubated with both uninfected and infected RBCs to rule out unspecific binding to the dye, but no signal was observed (Figure S4b,c).

2.4. Binding Assessment of Gold Nanoparticles to Different Asexual Stages of *P. falciparum*. As mentioned earlier, malaria parasites undergo maturation inside RBCs through rings, trophozoites, and schizonts. The binding efficacy was investigated in different erythrocytic stages. For this experiment, highly synchronized *P. falciparum* cultures were obtained using sorbitol, percoll, or magnetic separation. These synchronized cultures at specific life stages were incubated with ATTO@Glc-NCs, and binding was studied by CLSM and flow cytometry (FACS) analysis. ATTO@Glc-NCs bound all the asexual stages (rings, early and late trophozoites, and schizonts) of intracellular *P. falciparum*, according to CLSM (Figure 2c). FACS of highly synchronized cultures at 5% parasitemia showed that binding increased significantly from rings over trophozoites to schizonts as the parasitic membrane proteins with cysteine-rich domains increase (Figure 2b). Many *Plasmodium* membrane proteins are involved in RBC invasion and are most abundant during the later stages of intra-erythrocytic development.[23] ATTO@Glc-NCs did not significantly bind to uninfected RBCs.

Z-Stack confocal imaging was used to locate ATTO@Glc-NCs on and inside schizonts, as DAPI (in blue) co-localized with the tagged nanoclusters (in red) (Figure S5a). ATTO@Glc-NCs interacted with the surface and penetrated the parasite.

2.5. Binding Assessment of Gold Nanoparticles to *P. falciparum* Gametocytes. Malaria transmission occurs via the sexual blood stages, known as gametocytes. Gametocytogenesis can be induced in an *in vitro* culture under conditions that involve high parasitemia and low hematocrit to simulate

https://dx.doi.org/10.1021/acsami.0c09075
ACS Appl. Mater. Interfaces 2020, 12, 43380–43387

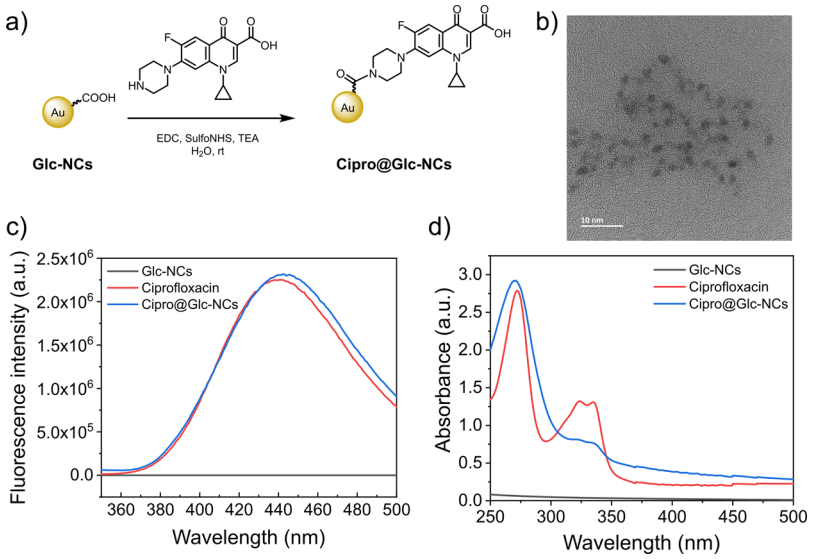

Figure 4. Synthesis and characterization of Cipro@Glc-NCs. (a) Synthetic scheme for the conjugation of ciprofloxacin to Glc-NCs leading to Cipro@Glc-NCs. (b) TEM imaging of Cipro@Glc-NCs revealed a nanoparticle size of 2 nm (scale bar: 10 nm). (c) Fluorescence spectroscopy showed an emission band at 450 nm for Cipro@Glc-NCs and ciprofloxacin but not for Glc-NCs. d) UV−Vis spectroscopy of Cipro@Glc-NCs revealed bands at 270, 325, and 335 nm corresponding to ciprofloxacin showing successful nanoparticle functionalization.

anemia and the presence of human serum and *N*-acetyl-glucosamine in the culture medium.[24,25] ATTO@Glc-NCs were incubated with intracellular sexual parasites using the same conditions described for asexual stages. CLSM was used to image the binding of ATTO@Glc-NCs to the different sexual stages. ATTO@Glc-NCs were able to bind to stages I−IV and even the isolated male and female gametocytes (stage V) that are responsible for malaria transmission via uptake by the mosquito during its meal (Figure 3). Stage IV gametocytes were analyzed by Z-stack imaging in confocal microscopy showing the interaction of ATTO@Glc-NCs with the surface and the inside of the parasite, as the signal of the tagged nanoclusters (in red) co-localized with the signal of the nuclei of the parasites (in blue) (Figure S5b).

2.6. Synthesis and Characterization of Ciprofloxacin-Conjugated Gold Nanoparticles. After showing that Glc-NCs selectively bind all *P. falciparum* blood stages but not to RBCs, we proceeded to study its ability to deliver drugs. Since Glc-NCs can traverse directly into the RBC and bind the parasite, they might show an improved inhibitory activity of drug−nanoparticle conjugates. We selected ciprofloxacin, an antibiotic that also has moderate antimalarial activity.[26] Ciprofloxacin derivatives show enhanced antimalarial activity when compared to the parent drug[27−30] and potentiate the effect of primaquine.[31] Ciprofloxacin is soluble in acetic acid but only slightly soluble in water and physiological buffers.[32] The presence of a carboxylic acid (p*K*a 6.0) and a secondary amine (p*K*a 8.8) provides two points for functionalization. The isoelectric point of the zwitterionic form of ciprofloxacin is 7.4 and, at this pH, the molecule is least soluble.[33] Conjugation of ciprofloxacin to Glc-NCs aims to bypass the zwitterionic state, reduce solubility problems, and ideally increase the therapeutic activity by intracellular delivery into the parasite. Glc-NCs were loaded with ciprofloxacin via the secondary amine to yield Cipro@Glc-NCs (Figure 4a). After purification, FT-IR analysis revealed the typical tertiary amide bond band at 1650 cm^{-1}, indicating that the reaction succeeded (Figure S6). TEM imaging showed that the nanoparticle size was 2 nm, demonstrating that Cipro@Glc-NCs were stable after drug conjugation (Figure 4b). The characteristic fluorescence emission band of ciprofloxacin at 450 nm (Figure 4c, red line) was visible in the Cipro@Glc-NCs sample (blue line) but not in Glc-NCs (black line), indicating that the nanoparticle loading succeeded. UV−Vis spectroscopy measurements further showed that the typical bands for ciprofloxacin at 272, 325, and 335 nm were also present in the Cipro@Glc-NCs sample (Figure 4d) and these bands could be further exploited for drug quantification. The loading of ciprofloxacin was quantified through a calibration curve, measuring the absorbance of different ciprofloxacin standards as well as the sample at 270 nm (Figure S7). The concentration of gold in the sample was measured by ICP-AES, indicating 0.8 μM ciprofloxacin/μM gold loading. The stability of Cipro@Glc-NCs was tested by overnight incubation in protein-rich growth medium. TEM imaging showed that the nanoparticle size ranged from 2 to 6 nm, indicating only a slight increase in size of some nanoparticles compared to the sample in water (Figure S2c). The fully characterized Cipro@Glc-NCs sample was used to inhibit *P. falciparum*.

2.7. Assessment of the Antimalarial Activity of Ciprofloxacin-Conjugated Gold Nanoparticles. The antimalarial activity of Cipro@Glc-NCs was compared to the free drug, incubating different concentrations of Cipro@Glc-NCs (concentration based on loaded ciprofloxacin), Glc-NCs, ciprofloxacin, and artemisinin (as a positive control) with *P. falciparum* for two life cycles (96 h). Parasitemia was assessed using the SYBR Green method,[34] quantified by fluorescence spectroscopy and further plotted as dose−response curves (Figure S8) to calculate IC_{50} values (Table 1). Glc-NCs did not show an inhibitory effect on the parasites, as no IC_{50} value could be obtained from the curves at the tested concentrations (Figure S8c). Cipro@Glc-NCs showed a significantly lower IC_{50} value (27.4 ± 3.8 μM) compared to ciprofloxacin alone (157.9 ± 58.8 μM), demonstrating the importance of directed drug delivery (Table S1). Even though the IC_{50} value of artemisinin (positive control) is 1000-fold lower than Cipro@Glc-NCs, the increasing resistance against this drug is a major problem and the development of new antimalarial therapeutics

https://dx.doi.org/10.1021/acsami.0c09075
ACS Appl. Mater. Interfaces 2020, 12, 43380−43387

Table 1. IC_{50} Values Obtained from Incubation of Cipro@Glc-NCs, Glc-NCs, Ciprofloxacin, and Artemisinin with *P. falciparum* for 96 h

sample	Cipro@Glc-NCs (μM)	ciprofloxacin (μM)	Glc-NCs (μM)	artemisinin (nM)
IC_{50}	27.4 ± 3.8	157.9 ± 58.8	n.d.[a]	14.9 ± 6.9

[a]n.d. = not determined.

is needed. The enhanced therapeutic activity of ciprofloxacin when using a nanoparticle formulation can be a result of the increased accumulation of the drug on or in the *P. falciparum* parasites in addition to the improved water solubility of ciprofloxacin, as the free drug forms aggregates in aqueous solutions.[35] Gold nanoparticles are attractive drug nanocarriers to specifically target cysteine-rich domains of surface proteins on protozoan parasites (e.g., *P. falciparum*) and improve the water solubility of hydrophobic drugs that lose efficacy as they form aggregates in aqueous media.

3. CONCLUSIONS

In conclusion, after showing that two different types of gold nanoparticles were able to bind extracellular *P. falciparum*, ultra-small, glucose-based gold nanoparticles were utilized to target all asexual and sexual erythrocytic stages of this protozoan parasite without unspecific binding or lysing RBCs. Gold nanoparticles likely interact with the protein via cysteine-rich domains of *P. falciparum* surface proteins. Ciprofloxacin-loaded nanoparticles rendered the moderate antimalarial drug more water-soluble and improved its efficacy against *P. falciparum* through a synergistic effect of selective targeting, leading to drug accumulation on the parasite, combined with better water solubility to prevent the formation of drug aggregates. Nanoparticle uptake into cells offers a significant advantage. Since these nanoparticles target all parasite stages, gameticidal effects may also block transmission. Minimal *in vitro* toxicity of glucose-based gold nanoparticles[22] and anti-parasitic activity demonstrate the potential of easy-to-synthesize gold nanoparticles as targeting devices. These findings might herald a paradigm shift in the field of antimalarials toward the use of gold nanoparticles as a multipurpose antiplasmodial agent.

4. EXPERIMENTAL SECTION

4.1. Materials. All reagents were commercially purchased and used without further purification. Ultrapure Millipore water (18.2 MΩ) was used as a solvent. All glassware was washed with Aqua Regia (HCl/HNO_3 in a 3:1 ratio by volume) and rinsed with ultrapure water. Gold(III) chloride solution (30 wt % in dilute HCl) and 1-thio-β-D-glucose sodium salt were purchased from Sigma Aldrich. RPMI was purchased from Pan Biotech.

4.2. Instruments. Transmission electron microscopy (TEM) measurements were performed on a Zeiss EM 912 Omega. The samples were prepared by immersion of grids into a small volume of the sample and subsequent solvent evaporation in a dust-protected atmosphere.

UV/Vis spectra were recorded on a Shimadzu UV-3600 spectrophotometer double-beam UV−VIS−NIR spectrometer and baseline-corrected.

ζ potential was measured using a Malvern Zetasizer instrument in order to obtain the electrophoretic mobility of nanoparticles at different times of dialysis against MilliQ water. The Helmholtz−Smoluchowski equation was used to correlate the measured electrophoretic mobilities to the zeta potentials. Three replicates of each sample were measured six times at 25 °C in MilliQ water.

Confocal microscopy imaging was performed with a Zeiss LSM 710 confocal microscope system equipped with a 63× magnification, numerical aperture 1.3 of Zeiss LCI Plan-NEOFLUAR water immersion objective lens (Zeiss GmbH, Germany).

Flow cytometry (FACS) analysis was acquired on a FACSCanto II flow cytometer (BD Biosciences, San Jose, CA, USA). The fluorescence of 10,000 living single cells was analyzed after monoparametric acquisition using an FITC height parameter (excitation with a 488 nm blue laser, 585/42 nm emission filter) and an APC height parameter (excitation with a 633 nm red laser, 660/20 nm emission filter). Data were analyzed with FlowJo analysis software (Tree Star Inc., Ashland, OR).

Inductively coupled plasma atomic emission spectrometry (ICP-AES) for gold concentration determination was performed on an Optima 8000, Perkin Elmer, Massachusetts, USA. Samples were diluted to a total volume of 5 mL using aqueous aqua regia. An external calibration series from 0.1 to 5 mg/L was prepared using Au standard solution. The average of three measurements was obtained, and the initial dilution was back calculated.

4.3. Synthesis. *4.3.1. Synthesis of Glucose-Based Gold Nanoclusters (Glc-NCs).* As reported elsewhere,[22] 1-thio-β-D-glucose sodium salt in MilliQ water (80.0 μL, 41.2 mM) was added to $HAuCl_4$ (1.0 mL, 2.9 mM) at room temperature. In a few seconds, a change in color from yellow to brownish was observed, indicating the formation of Glc-NCs. The solution was dialyzed in two cycles of 1.5 L of MilliQ water or filter-centrifuged using Amicon Ultra 15 mL tubes (3000*g*, 30 min, three times).

4.3.2. Synthesis of Citrate-Stabilized Gold Nanoparticles (Cit-AuNPs). As previously reported,[36] a preheated solution of sodium citrate (10 mL, 1%) in MilliQ water was added to a solution of $HAuCl_4$ (100 mL, 500 μM) in MilliQ water under boiling conditions (100 °C). No refluxing was used to prevent the presence of temperature gradients within the liquid. After 15 min, the red solution was cooled to room temperature. The resulting Cit-AuNPs were dialyzed against 1.5 L of MilliQ water three times.

4.3.3. Synthesis of ATTO-Tagged Glc-NCs (ATTO@Glc-NCs). A solution of Glc-NCs (5.0 mL, 1.4 μmol of Au, 6.11×10^{15} nanoclusters) was diluted with 25 mL of MilliQ water and 500 μL of PBS. To this solution, 1-ethyl-3-(3-dimethylaminopropyl)-carbodiimide (EDC, 6.5 mg, 34 μmol) and *N*-hydroxysulfosuccinimide (sulfo-NHS, 7.4 mg, 34 μmol) were added dropwise and the reaction was allowed to stir for 5 min under sonication in an ice bath. Subsequently, an aqueous solution of ATTO 647N dye (8.14 μL, 0.01 μmol) was added and allowed to react for 2 h under a cold sonication bath. The resulting ATTO@Glc-NCs were dialyzed against 1.5 L of MilliQ water three times.

4.3.4. Synthesis of Ciprofloxacin-Conjugated Glc-NCs (Cipro@Glc-NCs). Commercially available ciprofloxacin hydrochloride (1.4 mg, 4.2 μmol) was first stirred with trimethylamine (TEA, ∼1 μL, 8.4 μmol) to completely solubilize the drug. The carboxylic acid groups of Glc-NCs (0.42 μmol) were activated using 1-EDC (0.8 mg, 4.2 μmol) and sulfo-NHS (0.9 mg, 4.2 μmol) for 5 min at room temperature. To the activated Glc-NC solution in water, the mixture of ciprofloxacin and TEA was added and sonicated for 2 h. The resultant solution was dialyzed against MilliQ water overnight and filtered (0.45 μm filter) to obtain the ciprofloxacin-conjugated nanoparticles (Cipro@Glc-NCs).

4.4. Biological Assays. *4.4.1. Cultivation of P. falciparum 3D7.* *P. falciparum* 3D7 erythrocyte stages were cultured as previously reported.[37] The asexual growth medium was composed of RPMI 1640 supplemented with 2 mM L-glutamine, 5 mM HEPES buffer, 28 μg/mL hypoxanthine, 50 μg/mL gentamycin, and 0.5% AlbuMAX II. The no-*N*-acetyl-glucosamine gametocyte medium (NNGM) was composed of RPMI 1640 supplemented with 1 g of glucose, 28 μg/mL hypoxanthine, 25 mM HEPES, and 0.5% AlbuMAX II. The *N*-acetyl-glucosamine gametocyte medium (NGM) was composed of RPMI 1640 supplemented with 1 g of glucose, 28 μg/mL hypoxanthine, 25 mM HEPES, 5.8 g of *N*-acetyl-glucosamine, 0.5 mL of human serum, and 0.5% AlbuMAX II. Parasites were kept at 1% hematocrit in 150 cm^2 cell culture flasks at 37 °C under 5% CO_2.

https://dx.doi.org/10.1021/acsami.0c09075
ACS Appl. Mater. Interfaces 2020, 12, 43380−43387

Life cycle stages as well as parasitemia were determined daily by light microscopy. For the microscope slide preparation, 1 mL of resuspended culture was centrifuged for 5 min at 300*g* and the supernatants were removed. The sample was smeared on the glass slides by taking 7.5 μL of the blood pellet. The slides were then allowed to dry and were further fixed with methanol. The parasites were then stained with UN 1230 Giemsa staining solution, diluted to 6% (v/v) with staining buffer (7 mM phosphate, pH 7.1) for visualization under the microscope. The *P. falciparum* gametocyte stages were obtained by modification of a previously reported protocol.[25] Parasites were kept at 5% hematocrit in 10 cm Petri dishes at 37 °C under 5% CO_2, 5% O_2, 90% N_2, and 60% humidity.

For gametocyte induction, first asexual culturing and synchronization were required in order to initiate log growth during the first 10 days. This asexual culturing was followed by gametocyte induction by mimicking host anemia through total RBC replacement as well as by reducing the hematocrit from 5 to 1.25%. A further increase in % parasitemia also produced stressed parasites that induced gametocytogenesis. Once the gametocytes were induced, they were isolated depending on the early or late stage. Early-stage gametocytes were isolated by changing the asexual growth medium to NNGM and doing percoll synchronization in NGM. Late-stage gametocytes were isolated by changing the medium to NGM and doing percoll synchronization using NGM instead of the asexual growth medium. The gametocytes were then used for confocal microscopy imaging. Parasites were further kept at 5% hematocrit in 10 cm Petri dishes at 37 °C under 5% CO_2, 5% O_2, 90% N_2, and 60% humidity.

4.4.2. Sorbitol Synchronization of P. falciparum. Sorbitol synchronization allows for enrichment of ring-stage parasites in culture through lysis of most iRBCs containing mid and late trophozoites as well as schizonts. The parasite cultures were centrifuged for 5 min at 400*g*. The resulting pellet was resuspended in five times the pellet volume of sterile and preheated 5% sorbitol solution (in MilliQ water). Afterward, the cultures were incubated for 10 min at 37 °C and shaken every 3 min in a vortex mixer. Subsequently, the cultures were washed twice (400*g*, 10 min) with growth medium and transferred into a 150 cm^2 cell culture flask containing 60 mL of medium. Fresh RBCs were added to a final hematocrit of 1%.

4.4.3. Magnetic Cell Separation for Schizont Enrichment. Since the haem moiety in hemoglobin is diamagnetic, iRBCs containing only mature parasites can be separated using magnetic-activated cell sorting and LD columns. For this purpose, LD columns were placed on a magnetic column holder and equilibrated using 2 mL of parasite growth medium. The cultures were centrifuged at 300*g* for 5 min to obtain the parasite pellets that were then loaded on the column followed by 4 mL of growth medium. The flow through containing RBCs and ring-stage iRBCs was collected, and the column containing mature parasites was finally removed from the magnet and eluted with 2 mL of growth medium by applying pressure.

4.4.4. Percoll Synchronization of P. falciparum. Percoll synchronization allows for enrichment of mature-stage parasites (schizonts) in the culture in a similar way to magnetic cell separation. The parasite cultures were centrifuged for 5 min at 300*g*. A solution of percoll 70% in PBS was pre-warmed, and 1 mL of the pellet was gently deposited on top of this solution (using 15 mL Falcon tubes). This resulting mixture was subsequently centrifuged at 800*g* for 10 min at 37 °C, putting the acceleration and brake to minimum. The resulting red upper layer was collected as it contains mature parasites and washed extensively with growth medium (300*g*, 5 min). The culture was then transferred into the culture flask or plate by adjusting (when required) the hematocrit to 1%.

4.4.5. Saponin Isolation of P. falciparum Schizonts. Saponin treatment leads to complete lysis of RBCs and allows for the isolation of parasites. For this purpose, synchronized schizont stage cultures at very high parasitemia (>50%) were used. The cultures were therefore centrifuged (5 min, 400*g*) and resuspended in saponin solution (1 mL, 0.15%) and further incubated for 10 min in an ice bath, shaking the cultures every 3 min using a vortex mixer. The suspension was then centrifuged for 10 min at 2000*g*, maintaining the temperature at 4 °C, and the supernatant was discarded. The pellets were washed several times with ice-cold PBS until the supernatant became clear.

4.4.6. ICP-AES Analysis. Isolated mature parasites (by saponin) were thawed and washed with PBS (3000*g*, 5 min), and 500 μL of PBS was added to resuspend the pellet. Three different concentrations of Glc-NCs and Cit@AuNPs were used (5, 20, and 50 μM). For each experiment, 20 μL of the resuspended parasites was incubated with 1 mL of each gold nanoparticle solution in PBS for 15 min. The parasites were further washed three times with PBS (3000*g*, 5 min), and the pellet was treated with aqua regia and measured with ICP-AES.

4.4.7. Flow Cytometry. For parasitemia determination, as RBCs do not contain DNA, the iRBCs can be distinguished by using a DNA-staining dye (SYBR Green). For this purpose, 500 μL of a resuspended culture (containing 5 μL of RBCs) was centrifuged (300*g*, 5 min) and further washed with PBS. The pellet was then resuspended in 150 μL of PBS. Finally, 1 mL of PBS containing 4% PFA, 1 μL of the resuspended parasites, and a solution of SYBR Green (dilution, 1:10,000) were incubated for 20 min in the absence of light. Non-infected RBCs were used as a control. The measurements were performed using an FITC channel.

4.4.8. Binding Studies with ATTO@Glc-NCs. The parasitemia of a synchronized culture (rings, trophozoites, or schizonts) was determined as previously described, adjusting it to 1 and 10% parasitemia by adding fresh RBCs. The experiment was performed using both % parasitemia. Then, 500 μL of a resuspended culture (containing 5 μL of RBCs) and 5 μL of non-infected RBCs were centrifuged (300*g*, 5 min) and further washed with PBS. Subsequently, 1 mL of a dilution of ATTO@Glc-NCs (20 μM concentration based on Au) in growth medium and PBS was added to each sample. To prepare this solution, 500 μL of ATTO@Glc-NCs (40 μM concentration based on Au) was diluted with 500 μL of growth medium and 50 μL of 10× PBS. The diluted ATTO@Glc-NCs were incubated with the parasites for 15 min under shaking and in the dark. The parasites were then thoroughly washed three times with PBS (300*g*, 5 min) and finally resuspended in 150 μL of PBS. Subsequently, 1 mL of PBS containing 4% PFA, 1 μL of the resuspended parasites, and a solution of SYBR Green (dilution, 1:10,000) were incubated for 20 min in the absence of light. Non-infected RBCs were used as a control. The measurements were performed using an FITC channel to detect parasitemia and APC channel to detect ATTO@Glc-NCs. Non-infected RBCs (treated and not treated with ATTO@Glc-NCs) and iRBC not treated with ATTO@Glc-NCs were used as a control. Experiments were done in triplicates.

4.4.9. Confocal Microscopy. For confocal imaging binding studies of both asexual and sexual cultures, 500 μL of a resuspended culture (containing 5 μL of RBCs) and 5 μL of non-infected RBCs were centrifuged (300*g*, 5 min) and further washed with PBS. Subsequently, 1 mL of a dilution of ATTO@Glc-NCs (20 μM concentration based on Au) in growth medium and PBS was added to each sample. To prepare this solution, 500 μL of ATTO@Glc-NCs (40 μM concentration based on Au) was diluted with 500 μL of growth medium and 50 μL of 10× PBS. The diluted ATTO@Glc-NCs were incubated with the parasites for 15 min under shaking and protected from light. The parasites were then thoroughly washed three times with PBS (300*g*, 5 min) and finally fixed by incubation with 500 μL of PBS containing 4% PFA for 15 min. Parasites were then centrifuged one more time and resuspended in 30 μL of PBS. To this suspension, 30 μL of mounting solution containing DAPI was added and carefully mixed. Finally, 10 μL of this mixture was put on a glass slide, covered with a glass cover, and fixed with nail polish. Non-infected RBCs (treated and not treated with ATTO@Glc-NCs) and iRBCs not treated with ATTO@Glc-NCs were used as a control.

4.4.10. Hemolysis Assay. A 96-well plate containing RBCs (1% hematocrit) was incubated with serial dilutions of Glc-NCs in PBS (20, 10, 5, 2.5, 1.3, 0.6, and 0.3 μM; concentration based on Au) in triplicates for 96 h. The plate was then centrifuged (300*g*, 5 min), and 50 μL of the supernatants was put in a Greiner 96 V Bottom Transparent Polystyrol in triplicates. The absorbance at 540 nm was

https://dx.doi.org/10.1021/acsami.0c09075
ACS Appl. Mater. Interfaces 2020, 12, 43380−43387

read using a plate reader. Supernatants of RBCs treated with PBS (negative control) and saponin (positive control) were also measured.

4.4.11. Stability of Glc-NCs and Cipro@Glc-NCs in Growth Medium. Cipro@Glc-NCs (10 μg/mL) and Glc-NCs (10 μM) were incubated overnight in RPMI media containing FBS (5%). The samples were loaded on the TEM grids and subsequently washed by dumping them on top of a water droplet for 15 min. The samples were allowed to dry before TEM imaging.

4.4.12. Antimalarial Activity of Cipro@Glc-NCs against P. falciparum. The antimalarial activity of Cipro@Glc-NCs was determined following a procedure described elsewhere.[34] For a typical experiment, 50 μL of a *P. falciparum* culture at 1% parasitemia and 4% hematocrit was incubated with 50 μL of different concentrations of Cipro@Glc-NCs, ciprofloxacin, Glc-NCs, artemisinin (positive control), and water (negative control) in a 96-well plate at 37 °C for 96 h (two life cycles). Subsequently, 100 μL of lysis buffer (20 mM Tris (pH 7.5), 5 mM EDTA, 0.008% (W/V) saponin, and 0.08% (V/V) Triton X-100) containing SYBR Green (1:10,000) was added to each well and the plate was incubated for 3 h at room temperature in the dark. Fluorescence intensity was measured at 485 nm excitation and 528 nm emission using a Tecan microplate reader. Fluorescence intensity plotted over log(concentration) was fitted in OriginPro (OriginLab Corporation, Northampton, MA, USA) to a sigmoidal dose−response curve where the inflection point corresponds to the IC50 value.

■ ASSOCIATED CONTENT

Supporting Information

The Supporting Information is available free of charge at https://pubs.acs.org/doi/10.1021/acsami.0c09075.

Additional figures on hemolysis, UV−Vis, TEM, CLSM, FT-IR, calibration curves, calculations, and inhibition curves (PDF)

■ AUTHOR INFORMATION

Corresponding Author

Peter H. Seeberger − *Department of Biomolecular Systems, Max Planck Institute of Colloids and Interfaces, 14476 Potsdam, Germany; Department of Biology, Chemistry, Pharmacy, Freie Universität Berlin, 14195 Berlin, Germany;* orcid.org/0000-0003-3394-8466; Email: Peter.Seeberger@mpikg.mpg.de

Authors

Silvia Varela-Aramburu − *Department of Biomolecular Systems, Max Planck Institute of Colloids and Interfaces, 14476 Potsdam, Germany; Department of Biology, Chemistry, Pharmacy, Freie Universität Berlin, 14195 Berlin, Germany*

Chandradhish Ghosh − *Department of Biomolecular Systems, Max Planck Institute of Colloids and Interfaces, 14476 Potsdam, Germany*

Felix Goerdeler − *Department of Biomolecular Systems, Max Planck Institute of Colloids and Interfaces, 14476 Potsdam, Germany; Department of Biology, Chemistry, Pharmacy, Freie Universität Berlin, 14195 Berlin, Germany*

Patricia Priegue − *Department of Biomolecular Systems, Max Planck Institute of Colloids and Interfaces, 14476 Potsdam, Germany; Department of Biology, Chemistry, Pharmacy, Freie Universität Berlin, 14195 Berlin, Germany*

Oren Moscovitz − *Department of Biomolecular Systems, Max Planck Institute of Colloids and Interfaces, 14476 Potsdam, Germany; Department of Biology, Chemistry, Pharmacy, Freie Universität Berlin, 14195 Berlin, Germany*

Complete contact information is available at: https://pubs.acs.org/10.1021/acsami.0c09075

Author Contributions

‖S.V.A. and C.G. contributed equally to this work.

Notes

The authors declare no competing financial interest.

■ ACKNOWLEDGMENTS

The authors thank the Max-Planck Society for generous financial support. F.G. acknowledges funding by RTG 2046 "parasite infections". The authors thank Suzan Almeida and Rebeca Fortes-Martin for assistance on the parasite culture and Soeun Gim and Jeannette Steffen for support with ICP-AES measurements. Soeun Gim and Heike Runge are acknowledged for helping out with the TEM measurements.

■ REFERENCES

(1) World Health Organization. *World Malaria Report 2019*; World Health Organization: Geneva 2019.

(2) Cowell, A. N.; Winzeler, E. A. The Genomic Architecture of Antimalarial Drug Resistance. *Brief. Funct. Genomics* **2019**, *18*, 314−328.

(3) Marques, J.; Valle-Delgado, J. J.; Urbán, P.; Baró, E.; Prohens, R.; Mayor, A.; Cisteró, P.; Delves, M.; Sinden, R. E.; Grandfils, C.; de Paz, J. L.; García-Salcedo, J. A.; Fernàndez-Busquets, X. Adaptation of Targeted Nanocarriers to Changing Requirements in Antimalarial Drug Delivery. *Nanomed. Nanotechnol., Biol Med.* **2017**, *13*, 515−525.

(4) Santos-Magalhães, N. S.; Mosqueira, V. C. F. Nanotechnology Applied to the Treatment of Malaria. *Adv. Drug Delivery Rev.* **2010**, *62*, 560−575.

(5) Mhlwatika, Z.; Aderibigbe, B. Polymeric Nanocarriers for the Delivery of Antimalarials. *Molecules* **2018**, *23*, 2527−2542.

(6) Sanders, P. R.; Gilson, P. R.; Cantin, G. T.; Greenbaum, D. C.; Nebl, T.; Carucci, D. J.; McConville, M. J.; Schofield, L.; Hodder, A. N.; Yates, J. R., III; Crabb, B. S. Distinct Protein Classes Including Novel Merozoite Surface Antigens in Raft-like Membranes of Plasmodium Falciparum. *J. Biol. Chem.* **2005**, *280*, 40169−40176.

(7) Volz, J. C.; Yap, A.; Sisquella, X.; Thompson, J. K.; Lim, N. T. Y.; Whitehead, L. W.; Chen, L.; Lampe, M.; Tham, W.-H.; Wilson, D.; Nebl, T.; Marapana, D.; Triglia, T.; Wong, W.; Rogers, K. L.; Cowman, A. F. Essential Role of the PfRh5/PfRipr/CyRPA Complex during Plasmodium Falciparum Invasion of Erythrocytes. *Cell Host Microbe* **2016**, *20*, 60−71.

(8) Reddy, K. S.; Amlabu, E.; Pandey, A. K.; Mitra, P.; Chauhan, V. S.; Gaur, D. Multiprotein Complex between the GPI-Anchored CyRPA with PfRH5 and PfRipr Is Crucial for Plasmodium Falciparum Erythrocyte Invasion. *Proc. Natl. Acad. Sci.* **2015**, *112*, 1179−1184.

(9) Michon, P.; Stevens, J. R.; Kaneko, O.; Adams, J. H. Evolutionary Relationships of Conserved Cysteine-Rich Motifs in Adhesive Molecules of Malaria Parasites. *Mol. Biol. Evol.* **2002**, *19*, 1128−1142.

(10) Thompson, J.; Fernandez-Reyes, D.; Sharling, L.; Moore, S. G.; Eling, W. M.; Kyes, S. A.; Newbold, C. I.; Kafatos, F. C.; Janse, C. J.; Waters, A. P. Plasmodium Cysteine Repeat Modular Proteins 1−4: Complex Proteins with Roles throughout the Malaria Parasite Life Cycle. *Cell. Microbiol.* **2007**, *9*, 1466−1480.

(11) Sim, B. K. L.; Narum, D. L.; Chattopadhyay, R.; Ahumada, A.; Haynes, J. D.; Fuhrmann, S. R.; Wingard, J. N.; Liang, H.; Moch, J. K.; Hoffman, S. L. Delineation of Stage Specific Expression of Plasmodium Falciparum EBA-175 by Biologically Functional Region II Monoclonal Antibodies. *PLoS One* **2011**, *6*, No. e18393.

(12) Gilberger, T.-W.; Thompson, J. K.; Triglia, T.; Good, R. T.; Duraisingh, M. T.; Cowman, A. F. A Novel Erythrocyte Binding Antigen-175 Paralogue FromPlasmodium Falciparum Defines a New Trypsin-Resistant Receptor on Human Erythrocytes. *J. Biol. Chem.* **2003**, *278*, 14480−14486.

(13) van Dijk, M. R.; Janse, C. J.; Thompson, J.; Waters, A. P.; Braks, J. A. M.; Dodemont, H. J.; Stunnenberg, H. G.; van Gemert, G.-J.;

Sauerwein, R. W.; Eling, W. A Central Role for P48/45 in Malaria Parasite Male Gamete Fertility. *Cell* **2001**, *104*, 153−164.
(14) Ishino, T.; Chinzei, Y.; Yuda, M. Two Proteins with 6-Cys Motifs Are Required for Malarial Parasites to Commit to Infection of the Hepatocyte. *Mol. Microbiol.* **2005**, *58*, 1264−1275.
(15) Häkkinen, H. The Gold−Sulfur Interface at the Nanoscale. *Nat. Chem.* **2012**, *4*, 443−455.
(16) Acres, R. G.; Feyer, V.; Tsud, N.; Carlino, E.; Prince, K. C. Mechanisms of Aggregation of Cysteine Functionalized Gold Nanoparticles. *J. Phys. Chem. C* **2014**, *118*, 10481−10487.
(17) Chai, F.; Wang, C.; Wang, T.; Ma, Z.; Su, Z. L-Cysteine Functionalized Gold Nanoparticles for the Colorimetric Detection of Hg2+induced by Ultraviolet Light. *Nanotechnology* **2009**, *21*, 25501−25507.
(18) Luthuli, S. D.; Chili, M. M.; Revaprasadu, N.; Shonhai, A. Cysteine-Capped Gold Nanoparticles Suppress Aggregation of Proteins Exposed to Heat Stress. *IUBMB Life* **2013**, *65*, 454−461.
(19) Monti, S.; Carravetta, V.; Ågren, H. Decoration of Gold Nanoparticles with Cysteine in Solution: Reactive Molecular Dynamics Simulations. *Nanoscale* **2016**, *8*, 12929−12938.
(20) Li, Z. P.; Duan, X. R.; Liu, C. H.; Du, B. A. Selective Determination of Cysteine by Resonance Light Scattering Technique Based on Self-Assembly of Gold Nanoparticles. *Anal. Biochem.* **2006**, *351*, 18−25.
(21) Sudeep, P. K.; Joseph, S. T. S.; Thomas, K. G. Selective Detection of Cysteine and Glutathione Using Gold Nanorods. *J. Am. Chem. Soc.* **2005**, *127*, 6516−6517.
(22) Varela-Aramburu, S.; Wirth, R.; Lai, C.-H.; Orts-Gil, G.; Seeberger, P. H. Straightforward and Robust Synthesis of Monodisperse Surface-Functionalized Gold Nanoclusters. *Beilstein J. Nanotechnol.* **2016**, *7*, 1278−1283.
(23) Cowman, A. F.; Crabb, B. S. Invasion of Red Blood Cells by Malaria Parasites. *Cell* **2006**, *124*, 755−766.
(24) Saliba, K. S.; Jacobs-Lorena, M. Production of Plasmodium Falciparum Gametocytes in Vitro. *Methods Mol. Biol.* **2013**, *923*, 17−25.
(25) Duffy, S.; Loganathan, S.; Holleran, J. P.; Avery, V. M. Large-Scale Production of Plasmodium Falciparum Gametocytes for Malaria Drug Discovery. *Nat. Protoc.* **2016**, *11*, 976−992.
(26) Gaillard, T.; Madamet, M.; Tsombeng, F. F.; Dormoi, J.; Pradines, B. Antibiotics in Malaria Therapy: Which Antibiotics except Tetracyclines and Macrolides May Be Used against Malaria? *Malar. J.* **2016**, *15*, 556−566.
(27) Dahl, E. L.; Rosenthal, P. J. Multiple Antibiotics Exert Delayed Effects against the Plasmodium Falciparum Apicoplast. *Antimicrob. Agents Chemother.* **2007**, *51*, 3485−LP − 3490.
(28) Krishna, S.; Davis, T. M. E.; Chan, P. C. Y.; Wells, R. A.; Robson, K. J. H. CIPROFLOXACIN AND MALARIA. *Lancet* **1988**, *331*, 1231−1232.
(29) Divo, A. A.; Sartorelli, A. C.; Patton, C. L.; Bia, F. J. Activity of Fluoroquinolone Antibiotics against Plasmodium Falciparum in Vitro. *Antimicrob. Agents Chemother.* **1988**, *32*, 1182−1186.
(30) Goodman, C. D.; Su, V.; McFadden, G. I. The Effects of Anti-Bacterials on the Malaria Parasite Plasmodium Falciparum. *Mol. Biochem. Parasitol.* **2007**, *152*, 181−191.
(31) Soares, R. P. P.; Krettli, A. U.; de Souza, M. V. N.; Vasconcelos, T. R. A.; Boechat, N. Evaluation of Antimalarial and Fluoroquinolone Combinations against Plasmodium Falciparum in Vitro. *Int. J. Antimicrob. Agents* **2006**, *28*, 271−272.
(32) Sharma, P. C.; Jain, A.; Jain, S.; Pahwa, R.; Yar, M. S. Ciprofloxacin: Review on Developments in Synthetic, Analytical, and Medicinal Aspects. *J. Enzyme Inhib. Med. Chem.* **2010**, *25*, 577−589.
(33) Williams, D. A. Zwitterions and PH−Dependent Solubility. *Am. J. Heal. Pharm.* **1996**, *53*, 1732.
(34) Dery, V.; Duah, N. O.; Ayanful-Torgby, R.; Matrevi, S. A.; Anto, F.; Quashie, N. B. An Improved SYBR Green-1-Based Fluorescence Method for the Routine Monitoring of Plasmodium Falciparum Resistance to Anti-Malarial Drugs. *Malar. J.* **2015**, *14*, 481−487.
(35) Li, J.; Beuerman, R.; Verma, C. The Effect of Molecular Shape on Oligomerization of Hydrophobic Drugs: Molecular Simulations of Ciprofloxacin and Nutlin. *J. Chem. Phys.* **2018**, *148*, 104902.
(36) Turkevich, J.; Stevenson, P. C.; Hillier, J. A Study of the Nucleation and Growth Processes in the Synthesis of Colloidal Gold. *Discuss. Faraday Soc.* **1951**, *11*, 55−75.
(37) Radfar, A.; Méndez, D.; Moneriz, C.; Linares, M.; Marín-García, P.; Puyet, A.; Diez, A.; Bautista, J. M. Synchronous Culture of Plasmodium Falciparum at High Parasitemia Levels. *Nat. Protoc.* **2009**, *4*, 1899−1915.

https://dx.doi.org/10.1021/acsami.0c09075
ACS Appl. Mater. Interfaces 2020, 12, 43380−43387